Organic Electronics 24 (2015) 120–124

Contents lists available at ScienceDirect

Organic Electronics

journal homepage: www.elsevier.com/locate/orgel

The role of gap states on energy level alignment at an α-NPD/HAT(CN)$_6$ charge generation interface

Jin-Peng Yang [a,b,*], Fabio Bussolotti [d], Yan-Qing Li [c], Xiang-Hua Zeng [b], Satoshi Kera [a,d], Jian-Xin Tang [c], Nobuo Ueno [a,*]

[a] Graduate School of Advanced Integration Science, Chiba University, Chiba 263-8522, Japan
[b] College of Physical Science and Technology, Yangzhou University, Jiangsu 225009, China
[c] Institute of Functional Nano and Soft Materials (FUNSOM), Jiangsu Key Laboratory for Carbon-Based Functional Materials & Collaborative Innovation Center of Suzhou Nano Science and Technology, Soochow University, Suzhou 215123, China
[d] Institute for Molecular Science, Okazaki 444-8585, Japan

ARTICLE INFO

Article history:
Received 18 March 2015
Received in revised form 19 May 2015
Accepted 26 May 2015
Available online 27 May 2015

Keywords:
Gap states
Charge generation layer
Energy level alignment
Ultraviolet photoelectron spectroscopy

ABSTRACT

We report the effect of gap states on energy level alignment in a typical organic charge generation interface of N,N-bis(1-naphthyl)-N,N-diphenyl-1,1-biphenyl-4,4-diamine (α-NPD)/hexaazatriphenylene–hexacarbonitrile [HAT(CN)$_6$] by using ultraviolet and X-ray photoemission spectroscopy. The gap states tailed from the highest occupied molecular orbital (HOMO) onset of α-NPD dominate the Fermi level pinning at the α-NPD(<1.6 nm)/HAT(CN)$_6$ interface, which is favorable for charges generation upon bias operation and facilitates the electron injection from the HOMO-tail region of α-NPD to the lowest unoccupied molecular orbital (LUMO) region of HAT(CN)$_6$.

1. Introduction

In recent years, tandem organic light emitting diodes (Tandem OLEDs) have been attracting more attention for the development of next generation flat panel display and solid state lighting due to their advantages with flexibility, high efficiency, long lifetime, and low cost [1–3]. In tandem OLEDs, vertically stacked organic electroluminescent (EL) units are linked in series by charge generation layer (CGL), which is operated as charge generation and separation center and thus directly controls the final device performance e.g. current efficiency and power efficiency. The typical CGL used in tandem OLEDs has a bilayer structure, which usually consists of an organic–organic bilayer [4] or an organic–metal oxide bilayer [5], and the charge generation efficiency is governed by the offset of the highest occupied molecular orbital (HOMO) level of the donor layer and the lowest unoccupied molecular orbital (LUMO) level of the acceptor layer at the CGL interface [4–6]. However, a high drive voltage is always needed to ensure the efficient operation of tandem devices due to the existence of offset values in CGL, which usually lead a lower power efficiency rather than the single EL unit device [7–9]. To reduce these drive voltage losses in tandem OLEDs, smaller offset at the interface of the CGL is required. Thus, a comprehensive understanding of energy level alignment (ELA) is indispensable to elucidate the main reason of controlling these energy offsets in CGLs.

The electronic structures of typical CGLs have therefore been investigated recently to explain the working mechanism in tandem OLEDs according to the obtained energy diagrams.[4,11,12] Higher ionization potential inorganic materials (e.g. MoO_3, WO_3) and organic materials (e.g. HAT(CN)$_6$, F_{16}CuPc) are expected to be selected as a acceptor layer to further reduce the energy offset values to reach "ideal zero", since this goal requires that the electron affinities of these materials are larger than ionization potentials of donor layers. However, this "ideal zero" energy offset value has never been observed. Examples of energy offset on different charge generation layers are >0.4 eV for HAT(CN)$_6$/NPB [4], 0.4 eV for F_{16}CuPc/CuPc [10], 0.9 eV for WO_3/TCTA [11] and 0.8 eV for MoO_3/NPB [12]. These results give an open question of what's the key factor to determine the ELA at these CGLs and control the energy offset values. In particular, the ELA at the direct contacted interfaces of CGLs, which unfortunately is still under debating. For example, the integer charge transfer model proposed that electron/hole transfer induced polaron states should govern the ELA, and especially control the Fermi level pinning while the

* Corresponding authors at: Graduate School of Advanced Integration Science, Chiba University, Chiba 263-8522, Japan (J.-P. Yang and N. Ueno).
E-mail addresses: yangjp@yzu.edu.cn (J.-P. Yang), uenon@faculty.chiba-u.jp (N. Ueno).

http://dx.doi.org/10.1016/j.orgel.2015.05.033
1566-1199/

substrate work function is higher (or lower) than the ionization potential (or electron affinity (EA)) of organic films [13]. On the other hand, it was pointed out that band-gap states induced by structure defects [14,15] and impurities [16,17] control the Fermi level position in the energy gap of organic films, i.e., the Fermi level will be quasi-pinned at the position near the HOMO if the EA/work function of the substrate is greater than the ionization potential (IP)/work function of the organic film [18,19].

In this paper, organic CGL consisting of HAT(CN)$_6$ (a material with high EA, Fig. 1) and N,N-bis(1-naphthyl)-N,N-diphenyl-1,1-biphenyl-4,4-diamine (α-NPD) (a typical hole transport material, Fig. 1) is selected as a typical example in organic charge generation layers and the electronic structure of the CGL is studied by using ultraviolet and X-ray photoemission spectroscopy (UPS and XPS). The observed decrease in vacuum level (∼0.5 eV shift) and Fermi level pinning at 0.3 eV above α-NPD HOMO onset (α-NPD thickness range < ∼1.6 nm), namely at the energy where DOS of tailing states becomes to increase rapidly, directly proof the roll of these gap states that govern the ELA between HAT(CN)$_6$ and α-NPD at the interface region. The Fermi level pinning near the HOMO onset of the α-NPD is originated from the energy distribution of the gap states, which reduce the charge injection barrier. We therefore expect more favorable injection of electrons from HOMO region of α-NPD into LUMO region of HAT(CN)$_6$ films upon bias operation. Above 1.6-nm-thick α-NPD, the HOMO band bending of 0.6 eV is observed with the increase in α-NPD film thickness.

2. Experimental section

Photoemission experiments were performed in a Kratos AXIS UltraDLD ultrahigh vacuum surface analysis system, which consisted of an introduction chamber, molecular deposition chamber (pressure < 1×10^{-9} Torr), and analyzer chamber (the base pressure ∼5×10^{-10} Torr). ITO substrate (30 Ω/□) was first cleaned with acetone, ethanol, deionized water, and finally treated with UV-ozone before transferred into the chamber for molecular deposition. Molecular deposition and characteristization were carried out in two different chambers without breaking the vacuum. UPS spectra were acquired by using Helium discharge lamp with the photon energy ($h\nu$) of 21.22 eV. The resolution of the UPS measurement was 100 meV. XPS spectra were collected using a monochromatic Al Kα ($h\nu$ = 1486.6 eV) to study chemical reactions as well as core levels in the films. The resolution of XPS spectrum was 500 meV. In all the XPS and UPS spectra, the binding energy was referred to the Fermi level (E_F). The threshold ionization potential of all the films were obtained from HOMO onset position to secondary electron cut off (vacuum level) position. All UPS and XPS measurements were carried out at room temperature (298 K).

3. Results and discussion

The evolution of UPS spectra of incrementally deposited α-NPD on 15-nm-thick HAT(CN)$_6$ is shown in Fig. 2 as a function of the α-NPD thickness from 0 to 15 nm. With the thickness increase of α-NPD from 0.2 nm to 15 nm, the secondary electron cut off (SECO) progressively shifts to higher binding energy from 15.6 eV to 16.7 eV as shown in Fig. 2(a). Interestingly, the HOMO onset of α-NPD shows different thickness dependences in thickness regions of 0–1.6 nm (i) and over 1.6 nm (ii) (see Fig. 2(b) and (c)). Below the thickness of 1.6 nm (region i), α-NPD HOMO onset nearly stays unchanged at the binding energy of 0.3 eV. Above the thickness of 1.6 nm (region ii), the HOMO onset starts to gradually move to the higher binding energy side and finally saturates at 0.9 V when the thickness is above 12.8 nm, clearly demonstrating a band bending-like behavior. The same binding energy shift is also observed on other valence peaks of α-NPD in Fig. 2(b), i.e. HOMO-3 (marked with red arrow). The threshold ionization potential (IP_{th}) of the present 15-nm-thick α-NPD films is 5.4 eV, similar to other published results [20]. On the other hand, the HOMO onset of 15-nm-thick HAT(CN)$_6$ on ITO substrate is at 3.7 eV, with the IP_{th} of 9.3 eV, which agrees with the value reported by Christodoulou et al. [21], indicating the standing up orientation of HAT(CN)$_6$ in the present HAT(CN)$_6$ films.

Fig. 3 shows the thickness dependence of XPS spectra of (a) C 1s and (b) N 1s of α-NPD films on 15 nm HAT(CN)$_6$ on ITO substrate. In Fig. 3(a), C 1s peaks contributed by two different molecules can be easily distinguished. The peak at 287.2 eV is assigned to HAT(CN)$_6$ [22], while the peak at low binding energy of 284.4 eV (for 15-nm-thick α-NPD) is from α-NPD [23]. N 1s spectra in Fig. 3(b) also show N 1s peaks from HAT(CN)$_6$ and α-NPD. The N 1s peak at 400.3 eV comes from HAT(CN)$_6$, which consists of two N 1s components (—N═ group and C≡N group) [21]; and the peak at 399.6 eV is from α-NPD [24]. Moreover, no obvious new peaks are found in Fig. 3 between two molecules of HAT(CN)$_6$ and α-NPD, implying a weak interaction at this organic–organic interface. With increased α-NPD deposition, the intensities of C 1s and N 1s from HAT(CN)$_6$ are attenuated gradually with peak position shift of ∼0.1 eV (see Fig. S1 in Supplemental information [25]) The electron mean free path (λ_{mfp}) of the α-NPD film could be estimated to be 0.34 nm for C 1s photoelectron and 0.36 nm for N 1s photoelectron by using the ideal relation of observed attenuated intensity (I_{obs}) and the intensity before attenuation (I_0): $I_{obs} = I_0 \times \exp(-x_d/\lambda_{mfp})$ with the depth of photoionization/thickness of α-NPD (x_d). The electron mean free path here is much smaller than ∼2 nm measured for well-ordered PTCDA films on Ag(1 1 1) by Graber et al. [26], probably because α-NPD films are amorphous, which increase electron inelastic scattering and shorten the electron mean free path [32].

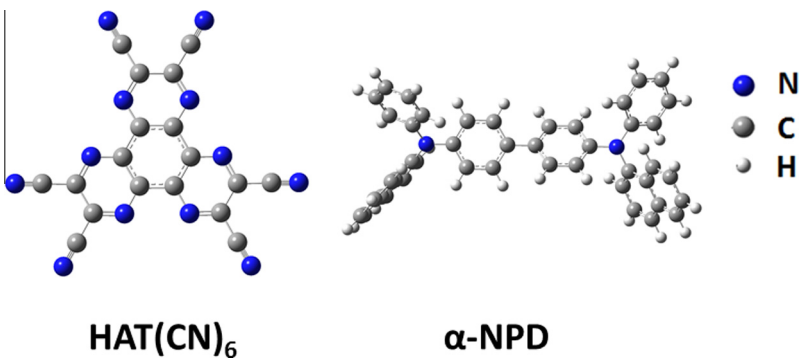

Fig. 1. Molecular sketch of HAT(CN)$_6$ ($C_{18}N_{12}$) and α-NPD ($C_{44}H_{32}N_2$).